J. Fluid Mech. (2020), *vol.* 882, A1. © Cambridge University Press 2019
doi:10.1017/jfm.2019.800

A note on forces exerted by a Stokeslet on confining boundaries

Viktor Škultéty[1] **and Alexander Morozov**[1,†]

[1]SUPA, School of Physics and Astronomy, The University of Edinburgh, James Clerk Maxwell Building, Peter Guthrie Tait Road, Edinburgh EH9 3FD, UK

(Received 8 May 2019; revised 13 September 2019; accepted 30 September 2019)

We consider a Stokeslet applied to a viscous fluid next to an infinite, flat wall, or in between two parallel walls. We calculate the forces exerted by the resulting flow on the confining boundaries, and use the results obtained to estimate the hydrodynamic contribution to the pressure exerted on boundaries by force-free self-propelled particles.

Key words: Stokesian dynamics, micro-organism dynamics, rheology

1. Introduction

Solutions to the Stokes equation can be constructed by combining suitably placed Stokeslets (the Green function of the Stokes equation) and other singular solutions, that simultaneously satisfy the equation of motion and the boundary conditions (Happel & Brenner 1983). This approach has proven especially fruitful in describing the motion of small solid bodies (Chwang & Wu 1975). In recent years, methods of Stokesian dynamics have been widely employed in studies of active matter systems and self-propelled particles (Lauga & Powers 2009; Spagnolie & Lauga 2012). Such systems often possess unique mechanical properties, with a vanishingly small shear viscosity observed in suspensions of swimming bacteria (López *et al.* 2015; Saintillan 2018) and a recent debate on the pressure exerted by microswimmers on the walls of the enclosing container (Takatori, Yan & Brady 2014; Yang, Manning & Marchetti 2014; Solon *et al.* 2015) being just a few examples. Most of the macroscopic properties predicted for active matter systems still await experimental confirmation. When designing such experiments, which typically include measurements of the forces that the system in question exerts on confining boundaries, as in the cases of shear viscosity and pressure, one often seeks to estimate the order of magnitude of the potential effect. Since the velocity fields generated by self-propelled particles can be constructed from the fundamental solutions of the Stokes equation, it is sufficient to consider the forces exerted on solid boundaries due to the latter. Surprisingly, there are no results available in the literature for the forces exerted on solid boundaries, even by the simplest of singularities, and here we seek to fill this gap.

We study two archetypal problems: a Stokeslet next to a single flat boundary, and a Stokeslet confined in between two parallel walls, see figure 1. Both problems

† Email address for correspondence: alexander.morozov@ed.ac.uk

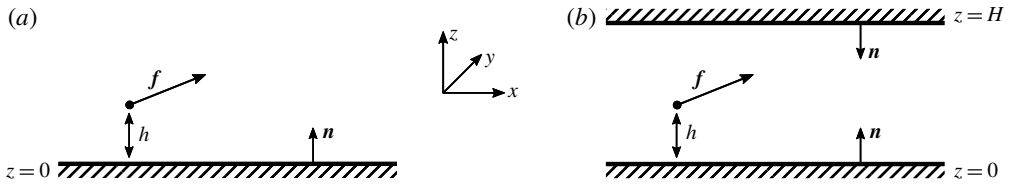

FIGURE 1. Geometries used in this note. (*a*) A point force applied to a fluid next to a wall. (*b*) A point force applied in between two parallel walls. The unit vector $\boldsymbol{n}$ gives the direction of the outer normal to each boundary.

are solved in a Cartesian coordinate system $\{x, y, z\}$, with the z-direction selected perpendicular to the boundaries. The velocity field $\boldsymbol{v}(\boldsymbol{r})$ at a position $\boldsymbol{r}$ satisfies the incompressible Stokes equation

$$-\partial_i p(\boldsymbol{r}) + \mu \partial^2 v_i(\boldsymbol{r}) + f_i \delta(\boldsymbol{r} - \boldsymbol{r_0}) = 0, \tag{1.1}$$

$$\partial_i v_i(\boldsymbol{r}) = 0, \tag{1.2}$$

where p is the pressure, and μ is the viscosity of the fluid; ∂_i denotes the spatial derivative in the ith direction, $i = \{x, y, z\}$, while ∂^2 denotes the Laplacian. The point force $\boldsymbol{f}$ is applied to the fluid at a position $\boldsymbol{r_0}$, which, without loss of generality, is chosen to be $(0, 0, h)$. The fluid is assumed to satisfy the no-slip condition at all boundaries. The solution to (1.1) and (1.2) has been obtained by Blake (1971), for the case of a single boundary, and by Liron & Mochon (1976) and Daddi-Moussa-Ider *et al.* (2018) for two confining walls. Here, we use these results to evaluate the associated forces applied by the fluid on the enclosing boundaries.

2. A point force next to a single boundary

In this problem, we consider a semi-infinite fluid bounded by an infinite, flat solid boundary at $z = 0$ (see figure 1*a*). The solution to (1.1) and (1.2) in this case has been obtained by Blake (1971), and reads

$$v_j = \frac{f_k}{8\pi\mu}\left[\left(\frac{1}{r} - \frac{1}{R}\right)\delta_{jk} + \frac{r_j r_k}{r^3} - \frac{R_j R_k}{R^3} + 2h\left(\delta_{k1}\frac{\partial}{\partial R_1} + \delta_{k2}\frac{\partial}{\partial R_2} - \delta_{k3}\frac{\partial}{\partial R_3}\right)\left\{\frac{hR_j}{R^3} - \frac{\delta_{j3}}{R} - \frac{R_j R_3}{R^3}\right\}\right], \tag{2.1}$$

$$p = \frac{f_k}{8\pi\mu}\left[\frac{r_k}{r^3} - \frac{R_k}{R^3} - 2h\left(\delta_{k1}\frac{\partial}{\partial R_1} + \delta_{k2}\frac{\partial}{\partial R_2} - \delta_{k3}\frac{\partial}{\partial R_3}\right)\left(\frac{R_3}{R^3}\right)\right], \tag{2.2}$$

where $\boldsymbol{r} = (x, y, z - h)$ and $\boldsymbol{R} = (x, y, z + h)$. An infinitesimal force exerted on the boundary by this velocity field is given by Landau & Lifshitz (1987),

$$\mathrm{d}F_i = \Sigma_{ij}|_{z=0}\, n_j \,\mathrm{d}x\,\mathrm{d}y, \tag{2.3}$$

where $\boldsymbol{n}$ is the outer normal to the solid boundary, and Σ_{ij} is the stress tensor

$$\Sigma_{ij} = -p\delta_{ij} + \mu(\partial_j v_i + \partial_i v_j). \tag{2.4}$$

Using $n_j = \delta_{jz}$, we obtain for the total force on the boundary

$$F_x = \mu \int_{-\infty}^{\infty} \mathrm{d}x\,\mathrm{d}y \partial_z v_x \Big|_{z=0}, \tag{2.5}$$

$$F_z = -\int_{-\infty}^{\infty} \mathrm{d}x\,\mathrm{d}y\, p \Big|_{z=0}, \tag{2.6}$$

where we used $\partial_x v_z|_{z=0} = \partial_y v_z|_{z=0} = 0$, since the operations of taking a derivative with respect to x or y and evaluating these velocity components at $z = 0$ commute, and v_i vanish at the boundary. In a similar fashion, we set $\partial_z v_z|_{z=0} = 0$ in (2.6), which follows from the incompressibility condition, equation (1.2), and the argument above. The expression for the y-component of the force is obtained by replacing the subscripts x with y in (2.5).

Explicit evaluation using (2.1) and (2.2) yields

$$\mu \partial_z v_x|_{z=0} = \frac{3hx}{2\pi} \frac{f_x x + f_y y - f_z h}{(h^2 + x^2 + y^2)^{5/2}}, \tag{2.7}$$

$$p|_{z=0} = \frac{3h^2}{2\pi} \frac{f_x x + f_y y - f_z h}{(h^2 + x^2 + y^2)^{5/2}}, \tag{2.8}$$

which, upon integration in (2.5) and (2.6), give

$$F_i = f_i. \tag{2.9}$$

The same conclusion can be reached by observing that the image system of a point force next to a flat no-slip boundary includes a Stokeslet of an equal and opposite strength and higher-order flow singularities (Blake 1971; Cichocki & Jones 1998; Bhattacharya & Bławzdziewicz 2002). The force on the wall is, therefore, equal to the force applied to the fluid. In § 4, we provide an intuitive argument for their equality.

3. A point force in a plane channel

In the second problem we consider a fluid confined in between two infinite parallel walls placed at $z = 0$ and $z = H$ (see figure 1*b*). The flow field $v_i(\boldsymbol{r})$ satisfies (1.1) and (1.2) with the boundary conditions $v_i(z = 0) = v_i(z = H) = 0$. The solution to this problem was first reported by Liron & Mochon (1976), who used a method similar to that of Blake (1971). An alternative approach was developed by Bickel (2007), and by Daddi-Moussa-Ider and co-workers (Daddi-Moussa-Ider & Gekle 2018; Daddi-Moussa-Ider *et al.* 2018), which is more convenient for evaluating the force applied to the boundaries. In what follows, we use the method of Daddi-Moussa-Ider *et al.* (2018), and repeat the main steps of their derivation for completeness. Since the result of Liron & Mochon (1976) is probably better known, in appendix A we repeat the same derivation using their method. We note here that the results of this analysis can also be deduced from the lubrication theory used to describe highly bidisperse colloidal suspensions (Bhattacharya & Blawzdziewicz 2008; Navardi & Bhattacharya 2010).

We start by introducing a two-dimensional Fourier transform for the velocity

$$v_i(x, y, z) = \frac{1}{(2\pi)^2} \int_{-\infty}^{\infty} \mathrm{d}k_x\,\mathrm{d}k_y \mathrm{e}^{\mathrm{i}(k_x x + k_y y)} \hat{v}_i(k_x, k_y, z), \tag{3.1}$$

and a similar transform for the pressure. Upon inserting these expressions into (1.1) and (1.2), we obtain

$$-\mathrm{i}k_\alpha \hat{p} + \mu(\partial_z^2 - k^2)\hat{v}_\alpha + f_\alpha \delta(z-h) = 0, \tag{3.2}$$

$$-\partial_z \hat{p} + \mu(\partial_z^2 - k^2)\hat{v}_z + f_z \delta(z-h) = 0, \tag{3.3}$$

$$\mathrm{i}k_x \hat{v}_x + \mathrm{i}k_y \hat{v}_y + \partial_z \hat{v}_z = 0, \tag{3.4}$$

where $\alpha = \{x, y\}$, and $k^2 = k_x^2 + k_y^2$. To proceed, we introduce the longitudinal and transverse components of the in-plane velocity

$$\hat{v}_x = \frac{k_x}{k}\hat{v}_l + \frac{k_y}{k}\hat{v}_t, \quad \hat{v}_y = \frac{k_y}{k}\hat{v}_l - \frac{k_x}{k}\hat{v}_t, \tag{3.5a,b}$$

and a similar transformation for the longitudinal f_l and transverse f_t components of the point force. Applying this transformation to (3.2)–(3.4), we obtain

$$\mu(\partial_z^2 - k^2)\hat{v}_t + f_t \delta(z-h) = 0, \tag{3.6}$$

$$-\mathrm{i}k\hat{p} + \mu(\partial_z^2 - k^2)\hat{v}_l + f_l \delta(z-h) = 0, \tag{3.7}$$

$$-\partial_z \hat{p} + \mu(\partial_z^2 - k^2)\hat{v}_z + f_z \delta(z-h) = 0, \tag{3.8}$$

$$\mathrm{i}k\hat{v}_l + \partial_z \hat{v}_z = 0. \tag{3.9}$$

These equations decouple the transverse component from the rest, and below we solve the associated problems separately.

3.1. *Transverse velocity component*

To solve (3.6), we observe that its solution can be split into two parts, $\hat{v}_t^+$ for $z > h$, and $\hat{v}_t^-$ for $z < h$, that satisfy that same equation

$$\mu(\partial_z^2 - k^2)\hat{v}_t^\pm = 0, \tag{3.10}$$

and the boundary conditions

$$\hat{v}_t^-(0) = \hat{v}_t^+(H) = 0. \tag{3.11}$$

The matching condition at $z = h$ is obtained by integrating (3.6) from $z = h - \varepsilon$ to $z = h + \varepsilon$, which, in the limit $\varepsilon \to 0$, yields

$$\partial_z \hat{v}_t^+(h) - \partial_z \hat{v}_t^-(h) = -f_t/\mu. \tag{3.12}$$

Together with the requirement that the velocity is continuous, $v_t^+(h) = v_t^-(h)$, this fully specifies the solution, which is given by

$$\hat{v}_t^-(z) = \frac{f_t}{k\mu}\frac{\sinh(k(H-h))}{\sinh(kH)}\sinh(kz), \tag{3.13}$$

$$\hat{v}_t^+(z) = \frac{f_t}{k\mu}\frac{\sinh(kh)}{\sinh(kH)}\sinh(k(H-z)). \tag{3.14}$$

3.2. *Longitudinal and vertical velocity components*

Excluding the pressure from (3.7) and (3.8), and using the incompressibility condition, equation (3.9), we obtain for the vertical velocity

$$\mu(\partial_z^2 - k^2)^2 \hat{v}_z - k^2 f_z \delta(z-h) - \mathrm{i}k f_l \partial_z \delta(z-h) = 0. \tag{3.15}$$

Similar to the transverse case, this equation is solved by splitting its solution into two components, $\hat{v}_z^{\pm}$, that satisfy

$$(\partial_z^2 - k^2)^2 \hat{v}_z^{\pm} = 0, \tag{3.16}$$

$$\hat{v}_z^-(0) = \partial_z \hat{v}_z^-(0) = \hat{v}_z^+(H) = \partial_z \hat{v}_z^+(H) = 0. \tag{3.17}$$

Repeated integration of (3.15) in a small vicinity of $z = h$ yields the following matching conditions

$$\partial_z^3 \hat{v}_z^+(h) - \partial_z^3 \hat{v}_z^-(h) = k^2 \mu^{-1} f_z, \tag{3.18}$$

$$\partial_z^2 \hat{v}_z^+(h) - \partial_z^2 \hat{v}_z^-(h) = \mathrm{i}k\mu^{-1} f_l, \tag{3.19}$$

$$\partial_z \hat{v}_z^+(h) - \partial_z \hat{v}_z^-(h) = 0, \tag{3.20}$$

$$\hat{v}_z^+(h) - \hat{v}_z^-(h) = 0. \tag{3.21}$$

The solution to (3.16)–(3.21) is given by

$$v_z^{\pm} = \frac{T_{zz}^{\pm} f_z + T_{zl}^{\pm} \mathrm{i}k f_l}{4k\mu(1 + 2H^2k^2 - \cosh(2Hk))}, \tag{3.22}$$

where

$$\begin{aligned} T_{zz}^-(z,h) \;=\; & -(2Hk^2(-h+H+z)+1)\sinh(k(h-z)) \\ & + k(z(4Hk^2(h-H)-1)+h-2H)\cosh(k(h-z)) \\ & + (2k^2(H-h)(H-z)+1)\sinh(k(h+z)) \\ & - k(h-2H+z)\cosh(k(h+z)) \\ & - (2hk^2z+1)\sinh(k(h-2H+z)) \\ & + k(h+z)\cosh(k(h-2H+z)) \\ & + \sinh(k(h-2H-z)) \\ & + k(z-h)\cosh(k(h-2H-z)), \end{aligned} \tag{3.23}$$

$$\begin{aligned} T_{zl}^-(z,h) \;=\; & (4Hk^2z(H-h)+(z-h))\sinh(k(h-z)) \\ & - 2Hk(h-H+z)\cosh(k(h-z)) \\ & + (h-z)\sinh(k(h+z)) \\ & + 2k(h-H)(H-z)\cosh(k(h+z)) \\ & + (z-h)\sinh(k(h-2H+z)) \\ & + 2hkz\cosh(k(h-2H+z)) \\ & + (h-z)\sinh(k(h-2H-z)), \end{aligned} \tag{3.24}$$

and

$$T_{zz}^+(z,h) = T_{zz}^-(H-z, H-h), \tag{3.25}$$

$$T_{zl}^+(z,h) = -T_{zl}^-(H-z, H-h). \tag{3.26}$$

The longitudinal component $\hat{v}_l$ can now be obtained from (3.9), while the pressure is given by (3.7).

3.3. *Forces exerted on the boundaries*

The forces applied by the flow determined above can now be calculated in a manner similar to § 2, and are given by

$$F_x^{\pm} = \mp\mu \int_{-\infty}^{\infty} \mathrm{d}x\,\mathrm{d}y\,\partial_z v_x^{\pm}, \tag{3.27}$$

$$F_z^{\pm} = \pm \int_{-\infty}^{\infty} \mathrm{d}x\,\mathrm{d}y\,p^{\pm}, \tag{3.28}$$

evaluated at $z = H$ and $z = 0$, respectively. Here, $v_x^{\pm}$ and $p^{\pm}$ are the inverse transforms of the corresponding Fourier components, and we used the fact that the outer normal at the $z = H$ boundary is pointing in the negative z-direction. The integrals in (3.27) and (3.28) can, in fact, be obtained from the Fourier transform introduced in (3.1). Indeed, if we put $k_x = k\cos\theta$ and $k_y = k\sin\theta$, for an arbitrary function ϕ that depends on x and y in a symmetric manner we obtain

$$\int_{-\infty}^{\infty} \mathrm{d}x\,\mathrm{d}y\phi(x, y) = \frac{1}{2\pi}\lim_{k\to 0}\int_0^{2\pi} \mathrm{d}\theta\hat{\phi}(k, \theta). \tag{3.29}$$

Therefore, the forces on the boundaries are readily obtained by integrating $\mp\mu\partial_z\hat{v}_x^{\pm}$ and $\pm\hat{p}^{\pm}$ over θ, taking the limit $k \to 0$ and evaluating the result at the appropriate z. The final results then read

$$F_\alpha^{-} = (1-\Delta)(1-\tfrac{3}{2}\Delta)f_\alpha, \quad F_z^{-} = (1-\Delta)^2(1+2\Delta)f_z, \tag{3.30a,b}$$

$$F_\alpha^{+} = \tfrac{1}{2}\Delta(3\Delta-1)f_\alpha, \quad F_z^{+} = \Delta^2(3-2\Delta)f_z, \tag{3.31a,b}$$

where $\Delta = h/H$, and $\alpha = \{x, y\}$.

4. Discussion

Equations (2.9) and (3.30)–(3.31) constitute the main results of this work. The first case corresponds to a Stokeslet near an infinite plane wall and implies that the whole force applied to the fluid is transmitted to the wall, independent of the Stokeslet's distance to the wall. While appearing surprising, this result can be understood from a simple argument. Due to the linearity of the Stokes equation, we expect the force on the wall to be proportional to the strength of the force applied to the fluid, $F_i = g(h)f_i$, where $g(h)$ is an unknown function of the distance between the Stokeslet and the wall. Since $g(h)$ should be dimensionless, it can only depend on a ratio between h and another length scale. However, there are no other length scales in the problem, and g is constant, independent of h. Considering the case when the Stokeslet is applied directly to the interface between the wall and the fluid fixes $g = 1$, giving the result in (2.9). An interesting consequence of this result is that an arbitrary force distribution applied to the fluid next to a single wall exerts no force on the wall, as long as the total force applied to the fluid is zero, as in the case of a collection of force-free self-propelled particles. In a similar fashion, a force-free microswimmer stalled by the wall, exerts no total force on it. Indeed, the propulsive force generated by the swimmer is directly transmitted to the wall through the action of the interaction potential between the wall and the swimmer. To generate this propulsive force, the

swimmer applies the equal and opposite force on the fluid some distance away from the wall, which is fully transmitted to the wall, as (2.9) suggests. The total sum is zero for any orientation of the swimmer in contact with the wall. Therefore, there is no hydrodynamic contribution to the pressure from a suspension of force-free swimmers next to a single boundary.

When the Stokeslet is confined between two parallel walls, the argument above yields $F_i = g(h/H)f_i$, since there are now two length scales in the problem. The corresponding functions g are non-trivial and different for the force components perpendicular and parallel to the wall, see (3.30) and (3.31). First, we observe that these expressions are symmetric with respect to $\Delta \to 1 - \Delta$, as expected. Next, in the limit of $H \to \infty$, keeping h finite, we recover (2.9) for the force on the lower wall, while $F_i^+ = 0$; the same holds for $h \to \infty$, keeping $H - h$ finite, with $F_i^+ = f_i$ and $F_i^- = 0$. Finally, the correct behaviour is also recovered in the limits of $h \to 0$ and $h \to H$.

Equations (3.30) and (3.31) also allow us to make an interesting observation regarding the total force applied to both boundaries. While the total vertical force on the walls is equal to the vertical force applied to the fluid, $F_z^- + F_z^+ = f_z$, the horizontal components give $F_\alpha^- + F_\alpha^+ = (1 - 3\Delta(1 - \Delta))f_\alpha$, with $\alpha = \{x, y\}$. The latter result implies that $F_\alpha^- + F_\alpha^+ \leqslant f_i$, where the equality only applies when $\Delta = 0$ or 1. To understand the origin of the 'missing' force, we consider an imaginary box around the Stokeslet and calculate the forces applied to the planes $x = \pm L$ and $y = \pm L$, where $L \gg H$. Far away from the Stokeslet, the velocity field is given by equation (51) of Liron & Mochon (1976), and has only the in-plane components, while the far-field behaviour of the pressure can be deduced from equation (56) of the same reference. Calculating the forces exerted by this velocity field in the x-direction on the fictitious surfaces as $L \to \infty$, we obtain that the forces at $y = \pm L$ are zero, while the forces at $x = \pm L$ are the same and equal to $(3/2)\Delta(1 - \Delta)f_x$, where only the pressure term contributes to this result. An identical expression is, of course, obtained for the y-component of the force, where only the fictitious surfaces perpendicular to the y-axis experience non-zero forces. Together with (3.30) and (3.31), this gives the total force applied to the boundaries enclosing the Stokeslet being equal to f_i, as it should.

We conclude by observing that our results can be trivially generalised for an arbitrary distribution of point forces applied to the fluid due to linearity of the Stokes equation. In particular, we consider a force dipole, which is relevant for force-free self-propelled microswimmers (Lauga & Powers 2009). The dipole consists of two equal and opposite point forces, $-f\boldsymbol{e}$ and $f\boldsymbol{e}$, applied to the fluid at $(0, 0, h)$ and $(0, 0, h) + l\boldsymbol{e}$, respectively, where f is the magnitude of the force, $\boldsymbol{e}$ is a unit vector along the direction of the dipole and l is its length. From (3.31), the vertical component force on the upper boundary due to the dipole is given by

$$F_d(h) = \frac{fl}{H}\left[-2\frac{l^2}{H^2}e_z^4 + 6e_z^2\Delta(1 - \Delta) + 3e_z^3\frac{l}{H}(1 - 2\Delta)\right], \tag{4.1}$$

where e_z denotes the z-component of $\boldsymbol{e}$. An equal and opposite force is applied to the lower boundary. Next, we consider a collection of such dipoles at a number density n. Although it has been demonstrated that suspensions of dipolar microswimmers exhibit significant correlations even at low densities (Stenhammar *et al.* 2017), here we assume the suspension to be homogeneous and isotropic, for simplicity. The pressure on the upper wall (a force per unit area) can then be calculated as the following

average

$$p_d = \frac{n}{2}\int_0^{\pi} \mathrm{d}\theta \sin\theta \int_0^{H} \mathrm{d}h F_d(h) \approx \frac{1}{3} f l n, \tag{4.2}$$

where we used $e_z = \cos\theta$ in spherical coordinates, and neglected terms of order l/H. Apart from a numerical factor, this result can be readily obtained from dimensional analysis. Using the dipolar strength $fl \sim 8 \times 10^{-19}$ N s as measured by Drescher *et al.* (2011) for *E.coli* bacteria, and setting $n \sim 10^9$ ml^{-1}, as in typical experiments with dilute bacterial suspensions (Jepson *et al.* 2013; López *et al.* 2015), we obtain $p_d \sim 10^{-4}$ Pa. Such pressures are too small to be measured by conventional rheometry but, perhaps, can be observed in an appropriate microfluidic experiment. We would like to note that the pressure calculated above is due to the velocity fields generated by the swimmers, and does not contain the osmotic contribution (Takatori *et al.* 2014; Yang *et al.* 2014; Solon *et al.* 2015).

Acknowledgements

Discussions with M. Cates, W. Poon, S. Spagnolie and J. Tailleur are gratefully acknowledged.

Appendix A. Alternative derivation of (3.30)–(3.31)

Here we demonstrate that the forces exerted on the walls of a plane channel by a Stokeslet can also be derived with the help of the velocity field obtained by Liron & Mochon (1976), which is probably the most famous treatment of that problem.

Their solution for the jth component of the velocity field due to the kth component of the point force, u_j^k, is decomposed into two parts

$$u_j^k = v_j^k + w_j^k, \tag{A 1}$$

where v_j^k is the contribution due to the original free-space Stokeslet, together with an infinite number of its images, and w_j^k is an auxiliary solution that ensures the no-slip boundary conditions at the walls. The Fourier transform of the auxiliary solution is given by equations (26) and (31) of Liron & Mochon (1976); note that their Fourier transform convention differs from ours, equation (3.1), by 2π. Using the same argument as in § 3.3, we express the contribution of the auxiliary solution to the forces on the upper boundary as

$$F_{w,\alpha}^{+} = -\mu f^k \lim_{\zeta\to\infty} \int_0^{2\pi} \mathrm{d}\theta\, \partial_z \hat{w}_\alpha^k(\lambda_x = \zeta\cos\theta,\, \lambda_y = \zeta\sin\theta,\, z = H), \tag{A 2}$$

$$F_{w,z}^{+} = f^k \lim_{\zeta\to\infty} \int_0^{2\pi} \mathrm{d}\theta\, \hat{p}^k(\lambda_x = \zeta\cos\theta,\, \lambda_y = \zeta\sin\theta,\, z = H), \tag{A 3}$$

where λ_x and λ_y are the analogues of k_x and k_y used in the main text, and $\zeta^2 = \lambda_x^2 + \lambda_y^2$, as in Liron & Mochon (1976). Here, $\alpha = \{x, y\}$, and $\hat{w}_\alpha^k$ and $\hat{p}^k$ denote the Fourier transforms of the auxiliary velocity and pressure, respectively. Performing the integrals and taking the limit yields

$$F_{w,\alpha}^{+} = -\tfrac{3}{2}\Delta(1-\Delta) f_\alpha, \tag{A 4}$$

$$F_{w,z}^{+} = -\Delta(1-\Delta)(1-2\Delta) f_z. \tag{A 5}$$

The velocity and pressure fields due to the original free-space Stokeslet and its images are given in equations (15) and (16) of Liron & Mochon (1976), and are conveniently expressed in terms of the infinite series from equations (43) and (44) *ibid.* Using (3.27) and (3.28), we obtain

$$F^{+}_{v,\alpha} = -\frac{f_\alpha}{2\pi H^2}\int_{-\infty}^{\infty} \mathrm{d}x\,\mathrm{d}y \times \sum_{n=1}^{\infty}(-1)^n \pi n \sin(\pi n \Delta)\left[\mathrm{K}_0\left(\frac{\pi n \rho}{H}\right) + \frac{x^2}{\rho}\frac{\pi n}{H}\mathrm{K}_1\left(\frac{\pi n \rho}{H}\right)\right] = f_\alpha \Delta, \quad (\mathrm{A}\,6)$$

$$F^{+}_{v,z} = -\frac{f_z}{\pi H^2}\int_{-\infty}^{\infty} \mathrm{d}x\,\mathrm{d}y \sum_{n=1}^{\infty}(-1)^n \pi n \sin(\pi n \Delta)\mathrm{K}_0\left(\frac{\pi n \rho}{H}\right) = f_z \Delta, \quad (\mathrm{A}\,7)$$

where $\rho^2 = x^2 + y^2$, K_0 and K_1 denote the zeroth- and first-order modified Bessel functions of the second kind, and we dropped the terms that do not contribute to the force. Combining these expressions with (A 4) and (A 5), we arrive at (3.31). The force on the lower boundary is obtained by replacing Δ with $1-\Delta$ in (3.31), as can be seen from (3.30).

REFERENCES

BHATTACHARYA, S. & BŁAWZDZIEWICZ, J. 2002 Image system for Stokes-flow singularity between two parallel planar walls. *J. Math. Phys.* **43** (11), 5720–5731.

BHATTACHARYA, S. & BLAWZDZIEWICZ, J. 2008 Effect of small particles on the near-wall dynamics of a large particle in a highly bidisperse colloidal solution. *J. Chem. Phys.* **128** (21), 214704.

BICKEL, T. 2007 Hindered mobility of a particle near a soft interface. *Phys. Rev.* E **75**, 041403.

BLAKE, J. R. 1971 A note on the image system for a Stokeslet in a no-slip boundary. *Math. Proc. Camb. Phil. Soc.* **70**, 303–310.

CHWANG, A. T. & WU, T. Y.-T. 1975 Hydromechanics of low-Reynolds-number flow. Part 2. Singularity method for stokes flows. *J. Fluid Mech.* **67**, 787–815.

CICHOCKI, B. & JONES, R. B. 1998 Image representation of a spherical particle near a hard wall. *Physica* A **258** (3), 273–302.

DADDI-MOUSSA-IDER, A. & GEKLE, S. 2018 Brownian motion near an elastic cell membrane: A theoretical study. *Eur. Phys. J.* E **41**, 19.

DADDI-MOUSSA-IDER, A., LISICKI, M., MATHIJSSEN, A. J. T. M., HOELL, C., GOH, S., BŁAWZDZIEWICZ, J., MENZEL, A. M. & LÖWEN, H. 2018 State diagram of a three-sphere microswimmer in a channel. *J. Phys.: Condens. Matter* **30**, 254004.

DRESCHER, K., DUNKEL, J., CISNEROS, L. H., GANGULY, S. & GOLDSTEIN, R. E. 2011 Fluid dynamics and noise in bacterial cell-cell and cell-surface scattering. *Proc. Natl Acad. Sci. USA* **108**, 10940–10945.

HAPPEL, J. & BRENNER, H. 1983 *Low Reynolds Number Hydrodynamics*, 2nd edn. Kluwer.

JEPSON, A., MARTINEZ, V. A., SCHWARZ-LINEK, J., MOROZOV, A. & POON, W. C. K. 2013 Enhanced diffusion of nonswimmers in a three-dimensional bath of motile bacteria. *Phys. Rev.* E **88**, 041002.

LANDAU, L. D. & LIFSHITZ, E. M. 1987 *Fluid Mechanics*, 2nd edn. Butterworth-Heinemann.

LAUGA, E. & POWERS, T. R. 2009 The hydrodynamics of swimming microorganisms. *Rep. Prog. Phys.* **72** (9), 096601.

LIRON, N. & MOCHON, S. 1976 Stokes flow for a stokeslet between two parallel flat plates. *J. Engng Maths* **10**, 287–303.

LÓPEZ, H. M., GACHELIN, J., DOUARCHE, C., AURADOU, H. & CLÉMENT, E. 2015 Turning bacteria suspensions into superfluids. *Phys. Rev. Lett.* **115**, 028301.

NAVARDI, S. & BHATTACHARYA, S. 2010 A new lubrication theory to derive far-field axial pressure difference due to force singularities in cylindrical or annular vessels. *J. Math. Phys.* **51** (4), 043102.

SAINTILLAN, D. 2018 Rheology of active fluids. *Annu. Rev. Fluid Mech.* **50** (1), 563–592.

SOLON, A. P., FILY, Y., BASKARAN, A., CATES, M. E., KAFRI, Y., KARDAR, M. & TAILLEUR, J. 2015 Pressure is not a state function for generic active fluids. *Nat. Phys.* **11**, 673–678.

SPAGNOLIE, S. E. & LAUGA, E. 2012 Hydrodynamics of self-propulsion near a boundary: predictions and accuracy of far-field approximations. *J. Fluid Mech.* **700**, 105–147.

STENHAMMAR, J., NARDINI, C., NASH, R. W., MARENDUZZO, D. & MOROZOV, A. 2017 Role of correlations in the collective behavior of microswimmer suspensions. *Phys. Rev. Lett.* **119**, 028005.

TAKATORI, S. C., YAN, W. & BRADY, J. F. 2014 Swim pressure: stress generation in active matter. *Phys. Rev. Lett.* **113**, 028103.

YANG, X., MANNING, M. L. & MARCHETTI, M. C. 2014 Aggregation and segregation of confined active particles. *Soft Matt.* **10**, 6477–6484.